Immunity. 2014 Feb 20;40(2):199-212.
doi: 10.1016/j.immuni.2013.12.014.

主論文

Autoimmune disorders associated with gain-of-function of the intracellular sensor MDA5

Masahide Funabiki[1,2,11], Hiroki Kato[1,3,4,11], Yoshiki Miyachi[2], Hideaki Toki[5], Hiromi Motegi[5], Maki Inoue[5], Osamu Minowa[5], Aiko Yoshida[6], Katashi Deguchi[6], Hiroshi Sato[7], Sadayoshi Ito[8], Toshihiko Shiroishi[9], Kunio Takeyasu[6], Tetsuo Noda[5,10], Takashi Fujita[1,3*]

[1]Laboratory of Molecular Genetics, Institute for Virus Research

[2]Department of Dermatology, Graduate School of Medicine

[3]Laboratory of Molecular Cell Biology, Graduate School of Biostudies

Kyoto University, 53 Shogoin-Kawaharacho, Sakyo-ku, Kyoto City, Kyoto 606-8507, Japan

[4]PrestoPrecursory Research for Embryonic Science and Technology (PRESTO), Science and Technology Agency (JST), Kawaguchi, Saitama 332-0012, Japan

[5]Team for Advanced Development and Evaluation of Human Disease Models, Riken BioResource Center (BRC), 3-1-1 Koyadai, Tsukuba, Ibaraki 305-0074, Japan

[6]Laboratory of Plasma Membrane and Nuclear Signaling, Graduate School of Biostudies, Kyoto University, Yoshida-konoe-cho, Sakyo-ku, Kyoto 606-8501, Japan

[7]Department of Clinical Pharmacology and Therapeutics, Tohoku University Graduate School of Pharmaceutical Sciences and Faculty of Pharmaceutical Sciences, 6-3 Aramaki-aza-aoba, Aoba-ku, Sendai 980-8578, Japan

[8]Division of Nephrology, Endocrinology and Vascular Medicine, Tohoku University Graduate School of Medicine, 1-1 Seiryo-cho, Aoba-ku, Sendai 980-8574, Japan

[9]Division of mammalian genetics laboratory, National Institute of Genetics, Yata 1111, Mishima, Shizuoka 411-8540, Japan

[10]Department of Cell Biology, Cancer Institute, The Japanese Foundation for Cancer Research, 3-8-31, Ariake, Koto, Tokyo 135-8550, Japan

[11]These authors contributed equally to this work.

*Corresponding author

Laboratory of Molecular Genetics, Institute for Virus Research, Kyoto University, 53 Shogoin-Kawaharacho, Sakyo-ku, Kyoto City 606-8507, Japan

Phone: +81-75-751-4031; E-mail: tfujita@virus.kyoto-u.ac.jp

SUMMARY

MDA5 is an essential intracellular sensor for several viruses, including picornaviruses, and elicits antiviral interferon (IFN) responses by recognizing viral dsRNAs. MDA5 has been implicated in autoimmunity. However, the mechanisms of how MDA5 contributes to autoimmunity remain unclear. Here we provide direct evidence that dysregulation of MDA5 caused autoimmune disorders. We established a mutant mouse line bearing MDA5 mutation by ENU mutagenesis, which spontaneously developed lupus-like autoimmune symptoms without viral infection. Inflammation was dependent on an adaptor molecule, MAVS indicating the importance of MDA5-signaling. In addition, intercrossing the mutant mice with type I IFN receptor-deficient mice ameliorated clinical manifestations. This MDA5 mutant could activate signaling in the absence of its ligand, but was paradoxically defective for ligand- and virus-induced signaling, suggesting that the mutation induces a conformational change in MDA5. These findings provide insight into the association between disorders of the innate immune system and autoimmunity.

INTRODUCTION

Innate immune responses including induction of type I interferon (IFNs) are initiated by receptors, which sense the invasion of microorganisms such as viruses and facilitate eradication of pathogens. Several transmembrane protein members, Toll-like receptors (TLRs), have been demonstrated to play an important role in antiviral responses by recognizing pathogen-specific molecular patterns (PAMPs) derived from viral species (Beutler, 2009; Imler and Hoffmann, 2001; Kawai and Akira, 2011) at the cell surface or in endosomes. In the cytoplasm, it has been shown that viral RNAs are sensed by RIG-I-like receptors (RLRs), which consist of three family member molecules, RIG-I, MDA5 and LGP2 (Yoneyama and Fujita, 2009). Cytosolic DNA also activates DNA sensors such as DDX41, IFI16 and cGAS to produce type I IFN (Sun et al., 2013; Unterholzner et al., 2010; Zhang et al., 2011).

RLRs are encoded by IFN-inducible genes and are expressed in various types of cells, including mouse embryonic fibroblasts (MEFs), dendritic cells (DCs) and macrophages. In conventional DCs (cDCs) RLRs play an essential role in antiviral defense, whereas TLRs play an essential role in plasmacytoid DCs (pDCs) for antiviral responses (Kato et al., 2005). These sensors discriminate non-self and self nucleic acids by their molecular structure in a sequence-independent manner. For instance, RIG-I is activated by double-stranded (ds) RNA and is also known to recognize RNAs with a tri-phosphate moiety at 5' end and/or polypyrimidine (Hornung et al., 2006; Pichlmair et al., 2006; Schlee et al., 2009; Takahasi et al., 2008). MDA5 also

detects dsRNA, such as poly(I;C), especially longer than 2 kbp in length (Kato et al., 2008).

Type I IFNs produced by the innate immune response, so called IFN responses, are the first line and major source of host antiviral defense. However, there is also an implication that excessive production of type I IFNs could rather cause a predisposition to autoimmunity (Trinchieri, 2010). There is also a murine model in which nucleic acid accumulates within cells, leading to excessive production of type I IFNs to cause autoimmunity (Yoshida et al., 2005). Some studies revealed the involvement of TLRs in autoimmunity. For example, TLR7 and TLR9 are important for autoantibody production in a murine model of lupus (Christensen et al., 2006), and spontaneous gene duplication of murine TLR7 causes a predisposition to autoimmunity (Pisitkun et al., 2006).

MDA5 (encoded by *IFIH1* in human) is associated with specific autoimmune diseases. A genome-wide association study (GWAS) revealed that single nucleotide polymorphisms (SNPs) of *IFIH1* (E627* and I923V), that are supposed to be a loss-of-function mutations (Shigemoto et al, 2009), are significantly associated with resistance to type 1 diabetes (Nejentsev et al., 2009). In amyopathic dermatomyositis patients, anti-CADM140 antibodies, which could potentially target MDA5, were detected in patients' sera (Nakashima et al., 2010). These findings imply a link between MDA5 and autoimmune diseases; however, the link remains to be determined and little is known about the specific mechanisms that lead to disease.

Here, we investigated the association of MDA5 with autoimmunity in a mouse model. We found that mutant mice, harboring a single missense mutation G821S in MDA5 generated by N-ethyl-N-nitrosourea (ENU) mutagenesis, spontaneously developed lupus-like nephritis and systemic autoimmune symptoms without viral infection. Here we provide direct evidence that dysregulation of an innate immune sensor, MDA5, causes autoimmune disorders.

RESULTS

ENU mutagenesis and identification of responsible gene

ENU mutagenesis and phenotype screenings were carried out as previously reported (Toki et al., 2013). Briefly, male C57BL/6JJcl (B6) mice were treated with ENU and then mated with DBA/2JJcl (D2) females. In the process of the dominant phenotype screenings in the F1 progeny, we detected a phenodeviants showing lupus-like nephritis. The inheritance of this phenotype was confirmed in N2 progeny backcrossed to D2, and the phenotype was mapped to 1.04-megabase (Mb) region in chromosome 5 (Figure S1A). We conducted genomic DNA sequencing of all exons and splice sites of all genes in this region. In consequence, one single-base substitution in exon 13 of *Ifih1*, resulting in amino acid exchange G821S (gs) was identified (Figure S1B). Thus, we concluded that this mutation was responsible for the phenotype. The F1 founder was backcrossed five generation to D2, and N6 progeny were subjected to a series of analyses.

Ifih1 gs mutant mice develop spontaneous inflammation in multi-organs

Major organs in mutant mice were analyzed histologically. Among several clinical manifestations, we found that nephritis was significant and reproducible in all heterozygous (*Ifih1*$^{gs/+}$) descendants, developing from 6 to 8 weeks after birth (Figures 1A and S1C) . In addition to nephritis, most *Ifih1* $^{gs/+}$ mice with a DBA/2 background developed severe multi-organ autoimmune disease. They showed growth retardation (Figure 1B) and 60 % of the mutant died within 24 weeks after birth (Figure 1C). There was mild infiltration of polymorphonuclear leukocytes in the haired skin of the forehead (Figure S1D). We also found calcification in the liver, which indicates chronic inflammation (Figure S1D). Of note, homozygotes developed more severe inflammation and rarely survived for 4 weeks after birth (data not shown). In the affected kidney, deposition of immunoglobulin and complement was observed (Figure 1D). Anti-nuclear antibodies (ANA) and anti-double-stranded (ds)-DNA antibodies were detected in the sera of *Ifih1*$^{gs/+}$ mice (Figure 1E). *Ifih1*$^{gs/+}$ mice developed hyperimmunoglobulinemia of all tested immunoglobulin classes (Figure 1F). These pathological and serological features were consistent with lupus-like nephritis. In the kidney, production of inflammatory cytokines and chemokines including IFN-β, IL-6, CXCL10, Isg56 and TNF-α was significantly upregulated (Figure 1G). Up-regulation of IFN-β and IL-6 in systemic organs was observed (Figure S1E), suggesting that chronic inflammation occurred in multiple organs, including the kidney of *Ifih1*$^{gs/+}$, although nephritis was especially evident. Consistent with the upregulation of IFN in multi-organs, increased mRNA of

RLRs as well as protein was detected (Figures S1F and S1G). In summary, the mice exhibit continued upregulation of IFN and IFN-stimulated genes in multiple organs.

Intrinsically activated DCs and macrophages are possible sources of chronic inflammation

MDA5 protein is ubiquitously expressed in multi-organs and various types of cells, including non-immune cells such as fibroblasts, and immune cells including DCs and macrophages. Abnormal function of innate immune cells are considered predisposing factors for systemic lupus erythematosus (SLE) as they produce robust type I IFNs as well as activating adaptive immune system to trigger autoimmunity (Liu and Davidson, 2012). To determine which cell types are responsible for systemic inflammation, we analyzed spleen cells by flow cytometry. *Ifih1*$^{gs/+}$ mice, both cDCs (CD11c^{hi}B220^{lo}) and pDCs (CD11c^{int}B220^{hi}) as well as macrophages (CD11b^{hi}F4/80^{int}) were increased in numbers and their cell surface marker, CD86, was upregulated (Figures 2A and 2B), suggesting that these DCs and macrophages are activated. Next, we sorted these cells and examined the induced amount of type I IFN and Cxcl10 (Figure 2C) as well as IL-6 (Figure S2A). As we expected, marked upregulation of these genes was detected in DCs and macrophages, whereas no upregulation was observed in T and B cells. Of note, when cDCs and macrophages were differentiated from bone marrow cells in the presence of GM-CSF, IFN induction and slight upregulation of

CD86 were clearly observed (Figure 2D and data not shown), suggesting that DCs and macrophages in *Ifih1*$^{gs/+}$ mice are activated intrinsically as well as through a bystander activation. Next we examined other cell types, including T cells and B cells. The ratio of T cells and B cells was normal in *Ifih1*$^{gs/+}$ splenocytes (Figure S2B). Effector ($CD44^{hi}CD62L^{lo}$) and memory ($CD44^{hi}CD62L^{hi}$) T cells were increased whereas naïve T ($CD44^{lo}CD62L^{hi}$) cells were decreased in *Ifih1*$^{gs/+}$ mice (Figure S2C). We detected upregulation of an activation marker CD69 in $CD4^+$ and $CD8^+$ T cells. Although no significant activation was observed in the B cell population by using the cell surface markers, GL7 and CD69 (Figure S2D), plasma cell population was slightly increased and absolute cell number was higher in *Ifih1*$^{gs/+}$ mice (Figure 2E), which could lead to augmentation of antibody production (Figures 1E and 1F). Consistent with systemic inflammation, granulocytes were significantly increased in *Ifih1*$^{gs/+}$ mice (Figures S2E and S2F). Thus, we identified DCs and macrophages were primary source of type I IFN and inflammatory cytokines, which could induce effector T cells and plasma cells, consequently leading to antibody production.

Hematopoietic cells are involved in nephritis

To access the contribution of hematopoietic cells to the chronic inflammation, we transferred bone marrow cells by reconstituting irradiated DBA/2 wild-type (WT) mice with *Ifih1*$^{+/+}$ or *Ifih1*$^{gs/+}$ bone marrow cells (Figure 3A). The mice with transferred bone marrow cells from *Ifih1*$^{gs/+}$ displayed nephritis (Figure 3B) and immunoglobulin deposition in the kidney (Figure 3C) beginning 6 weeks after reconstitution. In the kidney, significant

induction of inflammatory cytokines was detected (Figure 3D). In the spleen, upregulation of CD86 in both cDCs and pDCs was observed (Figure 3E). These results indicate that hematopoietic cells are sufficient for MDA5 mutation-dependent nephritis. Of note, those recipient mice exhibited a relatively milder phenotype than *Ifih1*$^{gs/+}$ mice, implicating that not only hematopoietic cells but also non-hematopoietic cells could possibly involved in MDA5 mutation-dependent nephritis.

Critical role of MAVS in the development of Nephritis in *Ifih1*$^{gs/+}$ mice

MAVS is the key adaptor molecule for the RLR pathway to transduce signaling downstream (Kawai et al., 2005; Meylan et al., 2005; Seth et al., 2005; Xu et al., 2005). To clarify the involvement of G821S MDA5 mutation in chronic inflammation, we intercrossed *Ifih1*$^{gs/+}$ mice with *Mavs*$^{-/-}$ mice with a C57BL/6 background. *Ifih1*$^{gs/+}$*Mavs*$^{+/-}$ mice developed nephritis with a less severe clinical score than *Ifih1*$^{gs/+}$•*Mavs*$^{+/+}$ mice (Figures 4A and 4B). In contrast, *Ifih1*$^{gs/+}$•*Mavs*$^{-/-}$ mice were devoid of nephritis and remained healthy. Moreover, production of type I IFNs and inflammatory cytokines in the kidney was revealed to be dependent on the gene dosage of *Mavs*; notably, virtually no production of these cytokines was detected in the absence of MAVS (Figure 4C). Consistent with our observation, virus-induced type I IFN production is reported to be dependent on *Mavs* gene dosage (Seth et al., 2005). Further, when CD11c^{+} cells in the spleen were examined, type I IFN gene expression observed in *Ifih1*$^{gs/+}$•*Mavs*$^{+/-}$ cells was abolished in *Ifih1*$^{gs/+}$•*Mavs*$^{-/-}$ cells (Figure 4D). Although the number of effector CD4^{+} T and effector CD8^{+} T cells was increased in the *Ifih1*$^{gs/+}$•*Mavs*$^{+/-}$ spleen

compared with the *Ifih1*$^{+/+}$•*Mavs*$^{+/-}$ spleen, additional deletion of the *Mavs* gene (*Ifih1*$^{gs/+}$•*Mavs*$^{-/-}$) abolished the increase of these effector cells (Figure S3A). In addition, activation of cDC and pDC as judged by the increase of CD86 expression, was similarly corrected by deletion of the *Mavs* gene (Figure S3B). These results strongly suggest that the observed kidney pathology, constitutive production of type I IFN and cytokines, and increase and activation of effector T cells and DCs are caused by a mutated *Ifih1* allele. Furthermore, the MDA5-MAVS axis is the key molecular basis for the pathogenesis in MDA5 gs mutant mice.

Type I IFN signaling contributes to but is not essential for MDA5-dependent nephritis

Emerging evidence has implicated dysregulated type I IFN production as a key predisposing factor for autoimmune diseases including SLE (Banchereau and Pascual, 2006). MDA5 signaling causes type I IFN induction as well as other cytokines. To further investigate the contribution of type I IFNs in the current autoimmune model, we intercrossed *Ifih1*$^{gs/+}$ mice with *Ifnar1*$^{-/-}$ mice on a C57BL/6 background. *Ifih1*$^{gs/+}$*Ifnar1*$^{-/-}$ mice had partially ameliorated nephritis; however, they still developed substantial pathology in the kidney (Figures 5A and 5B). In the affected kidney, slight induction of type I IFNs as well as inflammatory cytokines was observed (Figure 5C), suggesting that type I IFNs are partially responsible for the pathogenesis whereas the other inflammatory cytokines are potentially responsible for the pathology of MDA5 gs mutant mice.

G821S mutation of MDA5 is unresponsive to RNA ligands but costitutively active

We examined *Ifnb* expression in MEFs expressing the G821S MDA5 mutation. *Ifih1*$^{gs/gs}$ MEFs clearly expressed *Ifnb* gene in the absence of cellular stimuli and *Ifih1*$^{gs/+}$ MEFs exhibited lower, but significant upregulation compared to *Ifih1*$^{+/+}$ MEFs (Figure 6A), suggesting that the G821S mutation confers gain-of-function. To further confirm this notion, expression vectors for human MDA5 and its mutants were transiently expressed in cultured cells. In addition to G821S, which was conserved at the same amino acid position in human *IFIH1*, another mutation, A946T, which has been implicated in the relation with SLE, was tested (Gateva et al., 2009). Expression of human G821S as well as human A946T mutants strongly activated IFN-β promoter in Huh-7 cells (Figure 6B), suggesting that these mutations conferred intrinsic activation function on MDA5. Next to examine cell-type specificity in the mouse system, we introduced mutant MDA5 to *Ifih1*$^{-/-}$ DCs with retroviral vectors (Figure 6C). WT MDA5 expression resulted in constitutive expression of *Ifnb*, which is consistent with a previous notion that MDA5 exhibits constitutive activity when overexpressed. However, MDA5 gs exhibited significantly higher activity than the WT. These data indicate the importance of a conserved G821 region in mouse and human MDA5 to suppress auto-activation in both hematopoietic and non-hematopoietic cells. We next investigated IFN-β production in WT and mutant MEFs upon viral infection (Figures 6D and 6E). EMCV infection is exclusively detected by MDA5, whereas infection by

Newcastle disease virus (NDV) is exclusively detected by RIG-I (Kato et al., 2006). Upon EMCV infection, *Ifih1*$^{+/+}$ and *Ifih1*$^{gs/+}$ MEFs produced high levels of IFN-β; however, *Ifih1*$^{gs/gs}$ MEFs did not (Figure 6D). When these MEFs were infected with NDV, efficient production of IFN-β was observed due to the function of RIG-I in these cells (Figure 6E). Further, to clarify the response of A946T mutant, we introduced the mutant MDA5 to *Ifih1*$^{-/-}$ MEFs with expression vector and concluded that A946T could not respond to EMCV (Figure 6F). These results demonstrate that although G821S and A946T mutations confer constitutive activity, they disrupt responsiveness to viral infection.

G821S and A946T mutations lead to conformational change and abrogate ATPase activity of MDA5

To characterize the physicochemical properties of MDA5 gs and A946T, we produced recombinant MDA5 proteins. The purity of the recombinant MDA5 proteins was confirmed by SDS-PAGE (Figure 7A).First, the recombinant proteins were examined by an atomic force microscope (AFM) (Figure 7B). WT MDA5 appeared as three closely associated lumps, whereas MDA5 gs and A946T were observed as a single blunt lump. Quantification confirmed that MDA5 gs, A946T and WT have distinct molecular shapes, suggesting open and closed conformations, respectively. We next examined ATPase activity since MDA5 is a dsRNA-dependent ATPase (Sumpter et al., 2005). In the absence of dsRNA, WT MDA5 exhibited very low ATPase activity, which was markedly enhanced in the presence of polyI;C. In contrast, ATPase activity of neither MDA5 gs nor A946T was augmented even in the

presence of polyI;C (Figure 7C), consistent with the result that MDA5 gs and A946T failed to respond to viral infection (Figures 6D and 6F). Thus, the constitutive activity of MDA5 gs and A946T is likely a result of conformational alteration rather than hyper responsiveness to endogenous RNA ligand.

DISCUSSION

Type I IFNs are associated with a number of human autoimmune diseases including SLE. Here we described the molecular mechanisms of a type I IFN-mediated autoimmune disorder in a mouse model. We identified lupus-like features as well as up-regulation of type I IFNs and cytokines in multi-organs of MDA5 mutant mice. We showed that MAVS is essential for autoimmune disorders in MDA5 gs mice; thus, MDA5-dependent signaling through MAVS is critical for the pathogenesis of autoimmune disease associated with MDA5 mutation. Of note, MDA5 transgenic mice have been reported to upregulate the production of anti-nuclear antibodies in sera on an FcgR2b-deficient background, leading to glomerulonephritis (Crampton et al., 2012); however, MDA5 overexpression was not sufficient to develop autoimmune symptoms, suggesting that the magnitude of constitutive signaling by WT MDA5-overexpression is negligible compared to that by single copy of MDA5 gs. In accordance with this, no gene amplification but a point mutation of *IFIH1* has been implicated in human autoimmune diseases (Gateva et al., 2009).

It was surprising that the amount of IFN-β produced by *Ifih1*$^{gs/+}$ and *Ifih1*$^{gs/gs}$ cells was far lower than that produced upon viral infection. However, it was sufficient to cause severe symptoms in mice. We can explain this by hypothesizing a cell intrinsic mechanism: MDA5 gs possibly takes an auto-activated form even in the absence of RNA ligands, subsequently leading to constitutive signal transduction via MAVS. Consequently, it results in chronic activation of the type I IFN pathway through IRF3, IRF7,

NF-κB and MAP kinases, resulting in up-regulation of the genes of type I and III IFN, inflammatory cytokines and IFN-inducible genes.

Such chronic activation should take place in all cell types and is therefore sufficient to trigger biological consequences. This hypothesis is consistent with the result that deletion of MAVS but not IFNAR1 completely abrogated the pathology. Because hematopoietic *Ifih1*$^{gs/+}$ cell transfer is sufficient to reproduce the disorder, and DCs and macrophages up-regulate a cell activation marker, CD86, we propose DCs and macrophages as the primary cell types for initiating autoimmunity in *Ifih1*$^{gs/+}$ mice. The partial effect of type I IFN receptor deletion on rescue from the symptoms suggests the potential involvement of other inflammatory cytokines, including IL-6 and TNF-α, for amplifying the activation cascade, leading to the effector T cells and antibody production.

These observations suggest possible therapies targeting the pathway to arrest disease progression. For example, reagents that modify the molecular structure of MDA5 or direct blocking of the interaction between MDA5 and MAVS or inhibition of downstream kinases will provide fundamental therapy. Temporal depletion of DCs and macrophages would potentially ameliorate inflammation and tissue damage. Conversely, blocking ATPase activity of MDA5 gs and A946T would not provide therapeutic effect because gs and A946T are negative for ATPase activity.

Crystal structures of RIG-I suggest that free RIG-I has an open structure in which CARD is masked by interactions with helicase domain 2, thus being

inactive for signaling (Kowalinski et al., 2011). Upon binding with dsRNA, it markedly changes the conformation into a more packed structure, thereby releasing CARD. We propose a similar scenario for WT MDA5, which has an open structure with CARD masked; however, G821S mutation results in conformational change as revealed by AFM analysis.

Paradoxycally, in the response to viral infection, gs is unable to further up-regulate IFN. We propose that the gs mutation resulted in constitutive activity rather than being hypersensitive to endogenous RNA ligands. This hypothesis is supported by the observations; gs does not exhibit ATPase activity, even in the presence of dsRNA; AFM analysis revealed that purified gs protein takes distinct conformation from wild-type protein. It appears that gene induction by virus infection in WT cells is far more efficient than constitutive gene expression resulting from *Ifih1*$^{gs/+}$ mutation. This is possibly because WT MDA5 is efficiently activated by binding with viral dsRNA to form a fiber-like polymer to facilitate a signaling relay (Wu et al., 2013); however, MDA5 gs is activated without such polymerization.

Within human *IFIH1* SNPs, A946T has been reported to be a risk variant for SLE (Gateva et al., 2009). This missense mutation is implied to be a gain-of-function mutation in SLE (Robinson et al., 2011). We found that A946T, like G821S, constitutively activated IFN signaling. In addition, MDA5 A946T takes packed structure as observed by AFM and does not

exhibit ATPase activity even in the presence of dsRNA. These features resemble those of G821S. Consistent with our observation, it was reported that mutations in MDA5 helicase motif I, III and VI lead to constitutive IFN signaling with inactivation of ATPase activity (Bamming and Horvath, 2009). Furthermore, constitutive active mutants of RIG-I (mut1 and 2) exhibit no ATPase activity (Kageyama et al., 2011).

Increasing number of reports revealed that the molecules involved in innate immune signal pathways are associated with the development of inflammatory diseases. For example, NOD1 and NOD2, sense cytosolic peptidoglycan and muramyl dipeptide (MDP) respectively and activate MAPK and NF-κB dependent pathway (Elinav et al., 2011). Variants of NOD2 are reported to increase the susceptibility to Crohn's disease (CD) (Hugot et al., 2001; Ogura et al., 2001). These mutations abolish the ability to sense MDP and fail to activate NF-κB in peripheral blood mononuclear cells (van Heel et al., 2005), whereas overproduction of NF-κB regulated genes including TNF-α, IL-1β and IL-6 in epithelial cells and lamina propria macrophages are detected in CD patients. These paradoxical immune responses may resemble those mediated by MDA5 gs. In a basal state, MDA5 gs weakly but constitutively activates IFN signaling in the absence of ligand leading to persistent chronic inflammation. Conversely, in viral infection, MDA5 gs is defective in antiviral immune response for limiting inflammation, which could potentially underlie susceptibility to viral infection. For another inflammatory disease-associated molecule in NOD family, NALP-3 mutations are associated with three different

autosomal diseases, Muckle-Wells syndrome (MWS), chronic infantile neurological cutaneous and articular (CINCA) syndrome and familial cold autoinflammatory syndrome (FACS) (Bihl et al., 2005; Hoffman et al., 2001). These NALP-3 mutations result in an increased processing of pro-IL-1β and subsequent release of the active cytokine (Dinarello, 2004). These observations support gain-of-functional model for triggering chronic inflammation and provide a clue for understanding the mechanism of autoinflammatory disorders.

Some intracellular molecules that regulate degradation of nucleic acid have been linked to autoimmune disorders. For example, TREX1 is a major exonuclease that degradates endogenous DNA. In *Trex1*$^{-/-}$ mice, cell intrinsic ligands activate IFN signaling, consequently leading to autoimmunity (Gall et al., 2012; Stetson et al., 2008), linking the association that human genetic mutations in *Trex1* cause Aicardi-Goutieres syndrome (AGS) and chilblain lupus. In comparison, we defined MDA5 gs mutation as gain-of-function in basal state, but not hypersensitive to endogenous RNA ligands (above).

In summary, we describe the mechanisms of how MDA5 G821S mutation contributes to autoimmunity in a mouse model and how human SNP of MDA5 A946T potentially associates to autoimmune disorder. These findings provide novel insights into how dysregulation of cell-intrinsic antiviral sensors leads to autoimmunity and suggest approaches for therapeutic opportunities.

EXPERIMENTAL PROCEDURES

Mice

Ifih1$^{gs/+}$ mice with a DBA/2 background were proliferated by in vitro fertilization of *Ifih1*$^{gs/+}$ sperm × DBA/2JJcl female ovum. Heterozygotes of G821S MDA5 mutant with a DBA/2 background were analyzed as stated. Neither sex nor litter effects were detected by ANOVA in the survival rate and histological analysis and so data from different sexes and litters were analyzed together. *Mavs*$^{-/-}$ mice were kindly provided from S. Akira (Osaka University) and *Ifnar1*$^{-/-}$ mice were purchased from B&K Universal.

Cells, Virus and Reagents

MEFs were prepared from 12.5-13.5 embryos generated by in vitro fertilization of *Ifih1*$^{gs/+}$ ×*Ifih1*$^{gs/+}$ with a DBA/2JJcl background and cultured in Dulbecco's modified Eagle's medium (DMEM) with fetal bovine serum (FBS) and penicillin-streptomycin (100U/ml and 100μg/ml, respectively). To prepare GM-CSF-induced BMDCs, bone marrow cells were prepared from femora and tibia of 3- to 10-week-old mice. Cells were cultured in RPMI 1640 medium supplemented with 10% FBS, 100μM 2-ME, and 10 ng/ml murine GM-CSF (Peprotech). Medium was changed every 2 days. Encephalomyocarditis virus (EMCV) was purchased from ATCC.

Histological Analysis

Tissues were fixed in 10% formalin, paraffin embedded, cut into sections (5μm) and stained with hematoxylin-eosin or Periodic acid-Schiff.

Quantitative Real-Time PCR

Total RNA was prepared with TRIzol reagent (Invitrogen), treated with DNase I (Roche Diagnostics), and reverse-transcribed using a High-Capacity cDNA Reverse Transcription Kit (Applied Biosystems) according to the manufacturer's instructions. Reverse transcription-PCR was performed with the ABI PRISM 7700 sequence detection system (Applied Biosystems) or the STEP One plus Real Time PCR system (Applied Biosystems) and TaqMan Fast Universal PCR Master Mix (Applied Biosystems). TaqMan primers for mouse Ifnb1, IL-6, Cxcl10, Isg56, Tnfa and 18s rRNA were purchased from Applied Biosystems. The RNA copy numbers were normalized to that of internal 18s rRNA.

Flow Cytometry

Cell suspensions of the spleen were prepared by sieving and gentle pipetting, and were treated with red cell lysis. For surface staining, cells were maintained in the dark at 4 °C throughout. Cells were washed in ice-cold PBS, then incubated with each antibody for 15 min and washed twice with PBS. Antibodies for flow cytometry were purchased from BioLegend, eBioscience and BD Biosciences. Data were acquired on the FACS Canto II flow cytometer (BD Biosciences) and analyzed using FlowJo.

Bone Marrow Chimeras

WT mice with a DBA/2JJcl background were irradiated with 8Gy. Bone marrow cells from *Ifih1*$^{+/+}$ or *Ifih1*$^{gs/+}$ mice were infused i.v. 6 h

post-irradiation. Mice were treated with antibiotics for 12 d post-irradiation. To assess chimerism, we determined the abundance of WT and MDA5 mutant alleles in genomic DNA obtained from the spleen by PCR.

Plasmid Construct

The p-55 C1B Luc, pEF-BOS-FLAG MDA5 has been described previously (Shigemoto et al., 2009). pEF-BOS-FLAG-MDA5 G821S, A946T were constructed by introducing the mutations into pEF-BOS-FLAG MDA5 respectively using the KOD-Plus-Mutagenesis Kit (TOYOBO).

Retroviral expression

pLZR-IRES/GFP vector has been described previously (Satoh et al., 2010). A murine WT MDA5 or MDA5 G821S cDNA was cloned into the pLZR-IRES/GFP retroviral vector. The constructs were transfected into the packaging cell line PlatE, and viral supernatants were collected 48 hours after transfection.

Measurement of IFN-ß Production

Cells were infected with EMCV, NDV for the indicated period. Culture supernatants were collected and analyzed for IFN-ß with an enzyme-linked immunosorbent assay (ELISA). ELISA kit for mouse IFN-ß was purchased from PBL Biochemical Laboratories.

Luciferase Reporter Assay

The Dual-Luciferase Reporter Assay System (Promega) was used according to the manufacturer's instructions for luciferase assays. As an internal control, the Renilla Luciferase construct pRL-TK (Promega) was used.

Protein Purification

The cDNA encoding human WT MDA5, MDA5 G821S or A946T was inserted into pAcGHLT-B vector (BD Biosciences). To obtain recombinant baculoviruses, Sf9 insect cells were co-transfected with the expression plasmid and BD Baculo Gold Linearized Baculovirus DNA (BD Biosciences) according to the manufacturer's protocol. The recombinant MDA5 proteins were expressed in Sf9 or High five insect cells (2×10^7 cells/150 mm dish) by infection with recombinant baculovirus for 4 days. The cells were lysed in lysis buffer (50 mM Tris−HCl pH 8.0, 150 mM NaCl, 1.5 mM DTT, 1% Triton X-100) with protease inhibitor cocktail (Nacalai Tesque). The lysates were purified with Ni-NTA super-flow (QIAGEN) followed by glutathione Sepharose 4B (GE Healthcare) according to the manufactures' instructions.

ATPase Assay

Reaction mixture (25 µl: 1 µg purified recombinant protein, 100 ng RNA, 20 mM Tris–HCl pH 8.0, 1.5 mM $MgCl_2$, 1.5 mM DTT, 20 units Protector RNase Inhibitor (Roche), 1 mM ATP) was incubated at 37 °C for 30 min. The product, inorganic phosphate, was quantified using BioMol Green (Enzo).

AFM observation

AFM imaging of MDA5 was performed utilizing a Nanoscope IIIa/IV with a

type E or type J scanner (Digital Instruments Inc.) in air with the Tapping Mode at room temperature. The probes used were made of silicon crystal, and the cantilevers were 160 (± 20) μm in length with a spring constant of 12-103 Nm^{-1} (OMCL-AC160TS; Olympus). Images were captured with the height mode in a 512 × 512 pixel format at a scanning frequency of 2 Hz. The images obtained were plane-fitted and flattened with the computer program supplied in the imaging module. The three-dimensional surface plots of the pictures were also produced with this program. For observation by AFM, purified WT/mutant MDA5 was diluted in Tris buffer containing 20 mM Tris–Cl (pH 8.0), 1.5 mM $MgCl_2$, and 1.5 mM DTT, and was applied to a freshly cleaved mica surface pretreated with 10 mM spermidine. After 10 min, the mica was washed with water and dried with nitrogen gas.

ACKNOWLEDGMENT

This work was supported by independent grants from the Precursory Research for Embryonic Science and Technology (PRESTO), the Grant-in-Aid for Scientific Research from Japan Society for the Promotion of Science, Daiichi Sankyo Foundation of Life Science and the Takeda Science Foundation.

REFERENCES

Bamming, D., and Horvath, C.M. (2009). Regulation of signal transduction

by enzymatically inactive antiviral RNA helicase proteins MDA5, RIG-I, and LGP2. J Biol Chem *284*, 9700-9712.

Banchereau, J., and Pascual, V. (2006). Type I interferon in systemic lupus erythematosus and other autoimmune diseases. Immunity *25*, 383-392.

Beutler, B. (2009). Microbe sensing, positive feedback loops, and the pathogenesis of inflammatory diseases. Immunol Rev *227*, 248-263.

Bihl, T., Vassina, E., Boettger, M.K., Goldbach-Mansky, R., Seitz, M., Villiger, P.M., and Simon, H.U. (2005). The T348M mutated form of cryopyrin is associated with defective lipopolysaccharide-induced interleukin 10 production in CINCA syndrome. Ann Rheum Dis *64*, 1380-1381.

Christensen, S.R., Shupe, J., Nickerson, K., Kashgarian, M., Flavell, R.A., and Shlomchik, M.J. (2006). Toll-like receptor 7 and TLR9 dictate autoantibody specificity and have opposing inflammatory and regulatory roles in a murine model of lupus. Immunity *25*, 417-428.

Crampton, S.P., Deane, J.A., Feigenbaum, L., and Bolland, S. (2012). Ifih1 gene dose effect reveals MDA5-mediated chronic type I IFN gene signature, viral resistance, and accelerated autoimmunity. J Immunol *188*, 1451-1459.

Dinarello, C.A. (2004). Unraveling the NALP-3/IL-1beta inflammasome: a big lesson from a small mutation. Immunity *20*, 243-244.

Elinav, E., Strowig, T., Henao-Mejia, J., and Flavell, R.A. (2011). Regulation of the antimicrobial response by NLR proteins. Immunity *34*, 665-679.

Gall, A., Treuting, P., Elkon, K.B., Loo, Y.M., Gale, M., Jr., Barber, G.N., and Stetson, D.B. (2012). Autoimmunity initiates in nonhematopoietic cells and progresses via lymphocytes in an interferon-dependent autoimmune disease. Immunity *36*, 120-131.

Gateva, V., Sandling, J.K., Hom, G., Taylor, K.E., Chung, S.A., Sun, X., Ortmann, W., Kosoy, R., Ferreira, R.C., Nordmark, G., *et al.* (2009). A large-scale replication study identifies TNIP1, PRDM1, JAZF1, UHRF1BP1 and IL10 as risk loci for systemic lupus erythematosus. Nat Genet *41*, 1228-1233.

Hoffman, H.M., Mueller, J.L., Broide, D.H., Wanderer, A.A., and Kolodner, R.D. (2001). Mutation of a new gene encoding a putative pyrin-like protein causes familial cold autoinflammatory syndrome and Muckle-Wells syndrome. Nat Genet *29*, 301-305.

Hornung, V., Ellegast, J., Kim, S., Brzozka, K., Jung, A., Kato, H., Poeck, H., Akira, S., Conzelmann, K.K., Schlee, M., *et al.* (2006). 5'-Triphosphate RNA is the ligand for RIG-I. Science *314*, 994-997.

Hugot, J.P., Chamaillard, M., Zouali, H., Lesage, S., Cezard, J.P., Belaiche, J., Almer, S., Tysk, C., O'Morain, C.A., Gassull, M., *et al.* (2001). Association of NOD2 leucine-rich repeat variants with susceptibility to Crohn's disease. Nature *411*, 599-603.

Imler, J.L., and Hoffmann, J.A. (2001). Toll receptors in innate immunity. Trends Cell Biol *11*, 304-311.

Kageyama, M., Takahasi, K., Narita, R., Hirai, R., Yoneyama, M., Kato, H., and Fujita, T. (2011). 55 Amino acid linker between helicase and carboxyl terminal domains of RIG-I functions as a critical repression domain and determines inter-domain conformation. Biochem Biophys Res Commun *415*, 75-81.

Kato, H., Sato, S., Yoneyama, M., Yamamoto, M., Uematsu, S., Matsui, K., Tsujimura, T., Takeda, K., Fujita, T., Takeuchi, O., and Akira, S. (2005). Cell

type-specific involvement of RIG-I in antiviral response. Immunity *23*, 19-28.

Kato, H., Takeuchi, O., Mikamo-Satoh, E., Hirai, R., Kawai, T., Matsushita, K., Hiiragi, A., Dermody, T.S., Fujita, T., and Akira, S. (2008). Length-dependent recognition of double-stranded ribonucleic acids by retinoic acid-inducible gene-I and melanoma differentiation-associated gene 5. J Exp Med *205*, 1601-1610.

Kato, H., Takeuchi, O., Sato, S., Yoneyama, M., Yamamoto, M., Matsui, K., Uematsu, S., Jung, A., Kawai, T., Ishii, K.J.*, et al.* (2006). Differential roles of MDA5 and RIG-I helicases in the recognition of RNA viruses. Nature *441*, 101-105.

Kawai, T., and Akira, S. (2011). Toll-like receptors and their crosstalk with other innate receptors in infection and immunity. Immunity *34*, 637-650.

Kawai, T., Takahashi, K., Sato, S., Coban, C., Kumar, H., Kato, H., Ishii, K.J., Takeuchi, O., and Akira, S. (2005). IPS-1, an adaptor triggering RIG-I- and Mda5-mediated type I interferon induction. Nat Immunol *6*, 981-988.

Kowalinski, E., Lunardi, T., McCarthy, A.A., Louber, J., Brunel, J., Grigorov, B., Gerlier, D., and Cusack, S. (2011). Structural basis for the activation of innate immune pattern-recognition receptor RIG-I by viral RNA. Cell *147*, 423-435.

Liu, Z., and Davidson, A. (2012). Taming lupus-a new understanding of pathogenesis is leading to clinical advances. Nat Med *18*, 871-882.

Meylan, E., Curran, J., Hofmann, K., Moradpour, D., Binder, M., Bartenschlager, R., and Tschopp, J. (2005). Cardif is an adaptor protein in the RIG-I antiviral pathway and is targeted by hepatitis C virus. Nature *437*, 1167-1172.

Nakashima, R., Imura, Y., Kobayashi, S., Yukawa, N., Yoshifuji, H., Nojima, T., Kawabata, D., Ohmura, K., Usui, T., Fujii, T.*, et al.* (2010). The RIG-I-like receptor IFIH1/MDA5 is a dermatomyositis-specific autoantigen identified by the anti-CADM-140 antibody. Rheumatology (Oxford) *49*, 433-440.

Nejentsev, S., Walker, N., Riches, D., Egholm, M., and Todd, J.A. (2009). Rare variants of IFIH1, a gene implicated in antiviral responses, protect against type 1 diabetes. Science *324*, 387-389.

Ogura, Y., Bonen, D.K., Inohara, N., Nicolae, D.L., Chen, F.F., Ramos, R., Britton, H., Moran, T., Karaliuskas, R., Duerr, R.H.*, et al.* (2001). A frameshift mutation in NOD2 associated with susceptibility to Crohn's disease. Nature *411*, 603-606.

Pichlmair, A., Schulz, O., Tan, C.P., Naslund, T.I., Liljestrom, P., Weber, F., and Reis e Sousa, C. (2006). RIG-I-mediated antiviral responses to single-stranded RNA bearing 5'-phosphates. Science *314*, 997-1001.

Pisitkun, P., Deane, J.A., Difilippantonio, M.J., Tarasenko, T., Satterthwaite, A.B., and Bolland, S. (2006). Autoreactive B cell responses to RNA-related antigens due to TLR7 gene duplication. Science *312*, 1669-1672.

Robinson, T., Kariuki, S.N., Franek, B.S., Kumabe, M., Kumar, A.A., Badaracco, M., Mikolaitis, R.A., Guerrero, G., Utset, T.O., Drevlow, B.E.*, et al.* (2011). Autoimmune disease risk variant of IFIH1 is associated with increased sensitivity to IFN-alpha and serologic autoimmunity in lupus patients. J Immunol *187*, 1298-1303.

Satoh, T., Kato, H., Kumagai, Y., Yoneyama, M., Sato, S., Matsushita, K., Tsujimura, T., Fujita, T., Akira, S., and Takeuchi, O. (2010). LGP2 is a positive regulator of RIG-I- and MDA5-mediated antiviral responses. Proc

Natl Acad Sci U S A *107*, 1512-1517.

Schlee, M., Roth, A., Hornung, V., Hagmann, C.A., Wimmenauer, V., Barchet, W., Coch, C., Janke, M., Mihailovic, A., Wardle, G.*, et al.* (2009). Recognition of 5' triphosphate by RIG-I helicase requires short blunt double-stranded RNA as contained in panhandle of negative-strand virus. Immunity *31*, 25-34.

Seth, R.B., Sun, L., Ea, C.K., and Chen, Z.J. (2005). Identification and characterization of MAVS, a mitochondrial antiviral signaling protein that activates NF-kappaB and IRF 3. Cell *122*, 669-682.

Shigemoto, T., Kageyama, M., Hirai, R., Zheng, J., Yoneyama, M., and Fujita, T. (2009). Identification of loss of function mutations in human genes encoding RIG-I and MDA5: implications for resistance to type I diabetes. J Biol Chem *284*, 13348-13354.

Stetson, D.B., Ko, J.S., Heidmann, T., and Medzhitov, R. (2008). Trex1 prevents cell-intrinsic initiation of autoimmunity. Cell *134*, 587-598.

Sumpter, R., Jr., Loo, Y.M., Foy, E., Li, K., Yoneyama, M., Fujita, T., Lemon, S.M., and Gale, M., Jr. (2005). Regulating intracellular antiviral defense and permissiveness to hepatitis C virus RNA replication through a cellular RNA helicase, RIG-I. J Virol *79*, 2689-2699.

Sun, L., Wu, J., Du, F., Chen, X., and Chen, Z.J. (2013). Cyclic GMP-AMP synthase is a cytosolic DNA sensor that activates the type I interferon pathway. Science *339*, 786-791.

Takahasi, K., Yoneyama, M., Nishihori, T., Hirai, R., Kumeta, H., Narita, R., Gale, M., Jr., Inagaki, F., and Fujita, T. (2008). Nonself RNA-sensing mechanism of RIG-I helicase and activation of antiviral immune responses.

Mol Cell *29*, 428-440.

Toki, H., Inoue, M., Motegi, H., Minowa, O., Kanda, H., Yamamoto, N., Ikeda, A., Karashima, Y., Matsui, J., Kaneda, H.*, et al.* (2013). Novel mouse model for Gardner syndrome generated by a large-scale N-ethyl-N-nitrosourea mutagenesis program. Cancer Sci.

Trinchieri, G. (2010). Type I interferon: friend or foe? J Exp Med *207*, 2053-2063.

Unterholzner, L., Keating, S.E., Baran, M., Horan, K.A., Jensen, S.B., Sharma, S., Sirois, C.M., Jin, T., Latz, E., Xiao, T.S.*, et al.* (2010). IFI16 is an innate immune sensor for intracellular DNA. Nat Immunol *11*, 997-1004.

van Heel, D.A., Ghosh, S., Butler, M., Hunt, K.A., Lundberg, A.M., Ahmad, T., McGovern, D.P., Onnie, C., Negoro, K., Goldthorpe, S.*, et al.* (2005). Muramyl dipeptide and toll-like receptor sensitivity in NOD2-associated Crohn's disease. Lancet *365*, 1794-1796.

Wu, B., Peisley, A., Richards, C., Yao, H., Zeng, X., Lin, C., Chu, F., Walz, T., and Hur, S. (2013). Structural basis for dsRNA recognition, filament formation, and antiviral signal activation by MDA5. Cell *152*, 276-289.

Xu, L.G., Wang, Y.Y., Han, K.J., Li, L.Y., Zhai, Z., and Shu, H.B. (2005). VISA is an adapter protein required for virus-triggered IFN-beta signaling. Mol Cell *19*, 727-740.

Yoneyama, M., and Fujita, T. (2009). RNA recognition and signal transduction by RIG-I-like receptors. Immunol Rev *227*, 54-65.

Yoshida, H., Okabe, Y., Kawane, K., Fukuyama, H., and Nagata, S. (2005). Lethal anemia caused by interferon-beta produced in mouse embryos carrying undigested DNA. Nat Immunol *6*, 49-56.

Zhang, Z., Yuan, B., Bao, M., Lu, N., Kim, T., and Liu, Y.J. (2011). The helicase DDX41 senses intracellular DNA mediated by the adaptor STING in dendritic cells. Nat Immunol *12*, 959-965.

FIGURE LEGENDS

Figure 1. MDA5 G821S mutant mice spontaneously develop lupus-like autoimmune disorder.

(A) Histology of kidney from *Ifih1*$^{+/+}$ and *Ifih1*$^{gs/+}$ mice (Left panels, Haematoxylin-eosin staining; Right panels, PAS).

(B) Body weight change of *Ifih1*$^{+/+}$ and *Ifih1*$^{gs/+}$ male and female mice following time course. *Ifih1*$^{+/+}$ male, N=14 ; *Ifih1*$^{+/+}$ female, N=15 ; *Ifih1*$^{gs/+}$ male, N=12 ; *Ifih1*$^{gs/+}$ female, N=13

(C) Survival curve of *Ifih1*$^{+/+}$(N=30) and *Ifih1*$^{gs/+}$(N=28) mice in DBA/2JJcl background (upper) and of male(N=12) and female(N=16) *Ifih1*$^{gs/+}$ mice (lower). Statistical significance was determined by Logrank test. *$p<0.03$, NS; not significant

(D) Immunoglobulin and complement 3(C3) depositions on *Ifih1*$^{gs/+}$ kidney.

(E) Production of anti-nuclear antibodies (ANA) and anti-double-stranded DNA (anti-dsDNA) antibodies in *Ifih1*$^{gs/+}$ sera.

(F) Hypergammaglobulinemia in *Ifih1*$^{gs/+}$ mice. Serum immunogloblin levels are shown. Statistical significance in (E) and (F) was determined by Student's *t*-test. *$p<0.03$

(G) Amounts of mRNA in kidney for indicated genes were quantified by quantitative real-time PCR (qPCR). Mean relative expression against littermate wild-type kidney is shown with standard as mean ± SD of

duplicate samples of a representative from three independent experiments. Open histogram, *Ifih1*$^{+/+}$; closed, *Ifih1*$^{gs/+}$ kidney.

Figure 2. Intrinsically activated DCs and macrophages are possible sources of chronic inflammation.

(A and B) Splenocytes were stained with CD11c and B220 (A) or CD11b and F4/80 (B) after MACS depletion of $CD3^+$ and $CD19^+$ cells and analyzed by flow cytometry. pDCs and cDCs(A), macrophages(B) were additionally gated and their CD86 expression was accessed in histogram and quantification of mean fluorescent intensity (MFI) was quantified in bar graphs. Closed histogram, *Ifih1*$^{+/+}$; red open, *Ifih1*$^{gs/+}$. Statistical significance was determined by Student's *t*-test. *$p<0.03$

(C) Indicated immune cells were sorted from spleen and indicated mRNA expression levels were determined by qPCR. Data are shown as mean ±SD of duplicate samples of a representative from two independent experiments.

(D) Bone marrow derived dendritic cells were sorted by MACS on day 6 and their *Ifnb* mRNA expression levels were determined by qPCR.

(E) (Left) Splenocytes were stained with CD19 /CD138 and analyzed by FACS. (Right) Absolute cell counts of plasma cells were shown in bar graphs. Statistical significance was determined by Student's *t*-test. **$p<0.05$

Figure 3. Hematopoietic cells are involved in renal pathogenesis.

(A) Schematic diagram of bone-marrow transfer experiments.

(B) Histology of kidney from *Ifih1*$^{+/+}$ and *Ifih1*$^{gs/+}$ bone-marrow transferred mice (Left panels, Haematoxylin-eosin staining; Right panels, PAS).

(C) Immunoglobulin and C3 depositions on kidney from *Ifih1*$^{+/+}$ and *Ifih1*$^{gs/+}$ bone-marrow transferred mice.

(D) mRNA expression of kidney from *Ifih1*$^{+/+}$ and *Ifih1*$^{gs/+}$ bone-marrow transferred mice was determined by qPCR. Data are shown as mean ±SD of duplicate samples of a representative from three independent experiments. Open histogram, *Ifih1*$^{+/+}$ bone-marrow transferred; closed, *Ifih1*$^{gs/+}$ bone-marrow transfererred mice.

(E) Whole splenocytes were prepared and stained with CD11c and B220. pDCs and cDCs were gated(Left) and their CD86 expression was accessed in histogram(Middle) and quantification of mean fluorescent intensity (MFI) was quantified in bar graphs(Right). Closed histogram, *Ifih1*$^{+/+}$; red open, *Ifih1*$^{gs/+}$splenocytes. Statistical significance was determined by Student's *t*-test. *p<0.03

Figure 4. MAVS is critical for the development of nephritis in *Ifih1*$^{gs/+}$ mice.

(A) Histology of kidney from WT, *Ifih1*$^{gs/+}$・*Mavs*$^{+/-}$ or *Mavs*$^{-/-}$ mice (Left panels, Haematoxylin-eosin staining; Right panels, PAS)

(B) Histological scores and %sclerosis in kidney from WT, *Ifih1*$^{gs/+}$・*Mavs*$^{+/+}$, *Mavs*$^{+/-}$ or *Mavs*$^{-/-}$ mice were evaluated. Statistical significance was determined by Student's *t*-test. *p<0.03

(C) Indicated mRNA gene expression levels in kidney from WT, *Ifih1*$^{gs/+}$・*Mavs*$^{+/+}$, *Mavs*$^{+/-}$ or *Mavs*$^{-/-}$ mice were determined by qPCR. Littermate mice were subjected and data are shown as mean ±SD of duplicate samples of a representative from three independent experiments.

(D) CD11c^{+} cells were sorted from splenocytes of indicated mice and their

mRNA expression was determined by qPCR. Data are shown as mean ±SD of duplicate samples of a representative from three independent experiments.

Figure 5. Type I IFNs are partially responsible but not essential for MDA-5 dependent nephritis.

(A) Histology of kidney from WT, *Ifih1*$^{gs/+}$・*Ifnar1*$^{+/-}$ or *Ifnar1*$^{-/-}$ mice (Left panels, Haematoxylin-eosin staining; Right panels, PAS)

(B) Histological scores and %sclerosis in kidney from WT, *Ifih1*$^{gs/+}$・*Ifnar1*$^{+/+}$, *Ifnar1*$^{+/-}$ or *Ifnar1*$^{-/-}$ mice were evaluated. Statistical significance was determined by Student's *t*-test. *p<0.03

(C) Indicated mRNA gene expression levels in kidney from *Ifih1*$^{gs/+}$・*Ifnar1*$^{+/+}$, *Ifnar1*$^{+/-}$ or *Ifnar1*$^{-/-}$ mice were determined by qPCR. Littermate mice were subjected and data are shown as mean ±SD of duplicate samples of a representative from three independent experiments.

Figure 6. G821S mutation of MDA5 is unresponsive to RNA ligands but constitutively active.

(A) Basal *Ifnb* mRNA level in MEFs are shown. Data are shown as mean ± SD of duplicate samples. Statistical significance was determined by Student's *t*-test. *p<0.03, **p<0.05

(B) Huh7 cells were transfected with a reporter gene (p-55C1B Luc) and empty vector (BOS) or expression vectors for FLAG-tagged human MDA5 and MDA5 mutants. 48 hrs after the transfection, luciferase activity was determined and indicated protein expression was accessed in SDS-PAGE.

Statistical significance was determined by Student's *t*-test. *p<0.03

(C) *Ifnb* mRNA levels in GM-CSF induced DCs expressing WT MDA5 and MDA5 gs. The DCs were infected with retroviruses which introduce indicated genes and GFP independently. 48hrs after infection, they were sorted according to GFP expression by FACS and subjected to qPCR. Data are shown as mean ±SD of duplicate samples of a representative from two independent experiments. Indicated gene expression in GFP(+) cells was shown by reverse transcription PCR in the right panel. Statistical significance was determined by Student's *t*-test. *p<0.03

(D and E) IFN-ß concentration in culture supernatant from MEFs infected with various titer of EMCV(D) or NDV(E) for 24hrs were measured by ELISA. Data are shown as mean ± SD of duplicate samples of a representative from three independent experiments.

(F) *Ifih1*$^{-/-}$ MEFs were transfected with empty vector or expression vector for human WT MDA5 or MDA5 A946T and a reporter gene, p-55C1B Luc. 48 hrs after the transfection, the cells were infected with EMCV for 6hrs and IFN-ß promoter activity was determined. Statistical significance was determined by Student's *t*-test. *p<0.05

Figure 7. G821S and A946T mutations lead to conformational change and abrogate ATPase activity of MDA5.

(A) Purity of MDA5 recombinant protein by SDS PAGE.

(B) Single-molecule analyses of the wild-type and mutant MDA5 molecules by AFM. (Top) Images were obtained from 500 nm scans. (Middle) Four individual molecules each in the wild-type and mutant images are marked

by arrow heads and depicted in 100 nm zoomed in scales. (Bottom) Section analyses where 4 individual height features from the middle panels were superimposed, illustrating the height differences between the wild-type and mutant molecules.

(C) ATPase activity of wild-type and mutant MDA5. ATPase activity of the recombinant wild-type and mutant MDA5 proteins were determined in the absence or presence of polyI:C. Data are the mean ± SD of duplicate samples of a representative of three independent experiments.

Supplemental Figure S1. Identification of responsible gene and phenotypical analysis of the ENU-mutagenized mice. (supporting data for Figure 1)

(A) Genetic fine mapping of ENU-induced strain showing glomerular nephritis. The black boxes (■) represent heterozygosity of the B6 and D2 allele (BD), and the white boxes (□) represent homozygosity of the D2 allele (DD). The numbers of mutant animals that inherited each haplotype are shown at the bottom of each column.

(B) Domain structure of MDA5. ★ represents the location of the mutation. Lower panel shows the result of genomic direct sequencing for *Ifih1*$^{+/+}$ and *Ifih1*$^{gs/+}$ mice.

(C) Histological score of kidney from *Ifih1*$^{gs/+}$ in DBA/2JJcl background following time course. *$p<0.03$

(D) General appearance and histology of skin and liver.

(E) mRNA expression of *Ifnb* and *Il6* from major organs were determined by qPCR. Data are shown as mean ± SD of duplicate samples of a representative from three independent experiments.

(F) mRNA expression of RLRs in kidney was determined by qPCR. Data are shown as mean ±SD of duplicate samples of a representative from three independent experiments.
(G) Protein expression of RLRs in liver, kidney and spleen was analyzed by SDS-PAGE.

Supplemental Figure S2. Flow cytometric analysis of the spleen in *Ifih1*$^{gs/+}$ mice. (supporting data for Figure 2)
(A) Indicated immune cells were sorted from spleen and *Il6* mRNA expression level was determined by qPCR. Data are shown as mean ±SD of duplicate samples of a representative from two independent experiments.
(B-F) Flow cytometric analysis of splenocytes. Expression of CD3 and B220 in splenic lymphocytes (B), expression of CD44 and CD62L in splenic CD4$^+$(upper) or CD8$^+$(lower) cells (C), expression of GL7 or CD69 in CD19$^+$ cells, expression of Gr-1 and Ter119 in splenocytes (E), expression of CD11b and Gr-1 in splenocytes (F).

Supplemental Figure S3. Abrogated inflammation in the spleen of *Ifih1*$^{gs/+}$・*Mavs*$^{-/-}$ mice. (supporting data for Figure 4)
(A and B) Flow cytometric analysis of splenocytes. Expression of CD44 and CD62L in splenic CD4$^+$ (upper) or CD8$^+$ (lower) cells (A), CD86 expression in splenic DCs (B). Similar results were obtained in three independent experiments.

Figure 1.

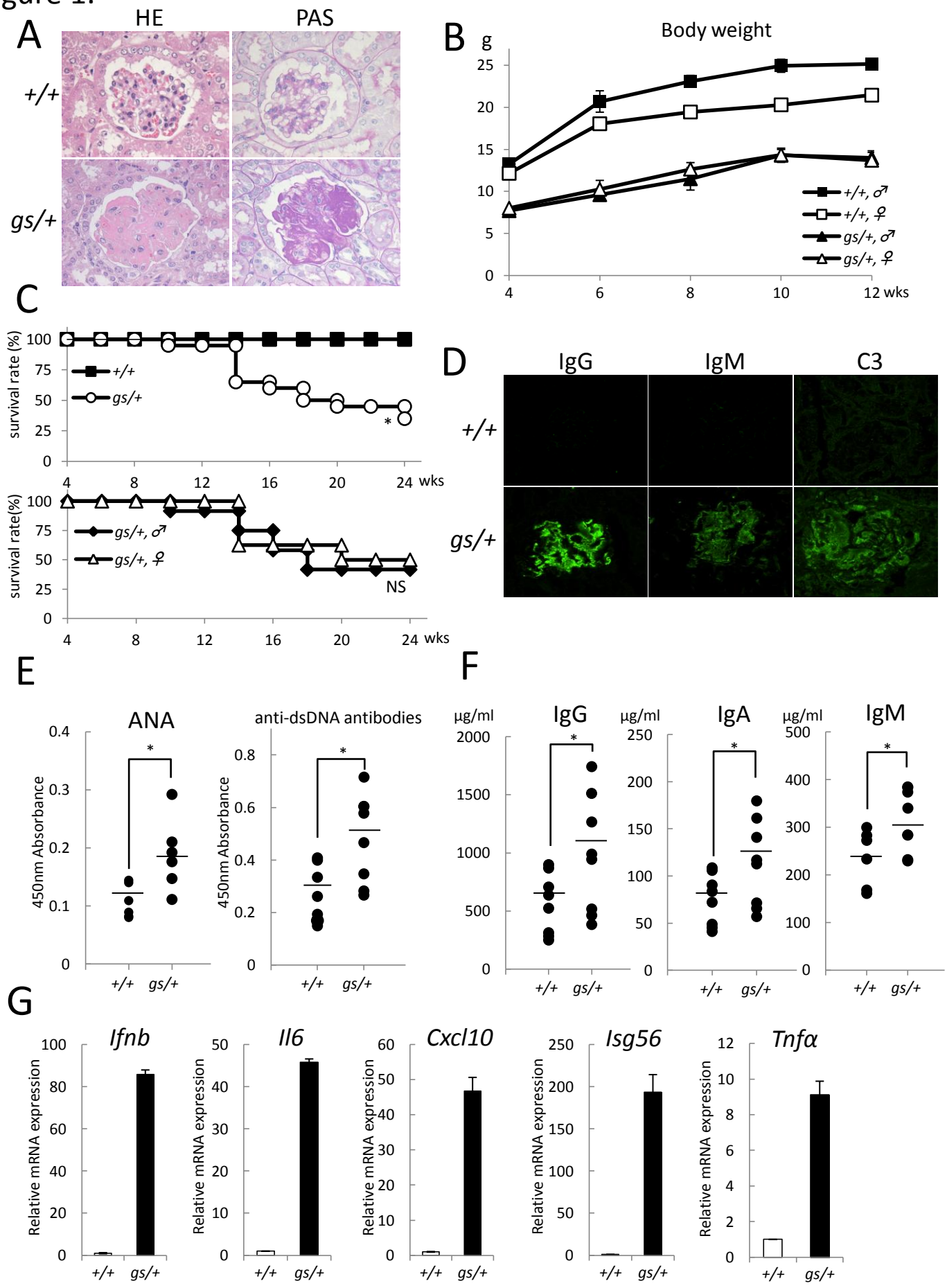
A
HE
PAS
+/+
gs/+
B
Body weight
g
25
20
15
10
5
0
4
6
8
10
12 wks
+/+, ♂
+/+, ♀
gs/+, ♂
gs/+, ♀
C
survival rate (%)
100
75
50
25
0
+/+
gs/+
*
4
8
12
16
20
24 wks
survival rate(%)
gs/+, ♂
gs/+, ♀
NS
D
IgG
IgM
C3
+/+
gs/+
E
ANA
anti-dsDNA antibodies
450nm Absorbance
0.4
0.3
0.2
0.1
0
0.8
0.6
+/+
gs/+
F
IgG
IgA
IgM
μg/ml
2000
1500
1000
500
250
200
150
100
50
500
400
300
G
Ifnb
Il6
Cxcl10
Isg56
Tnfα
Relative mRNA expression
100
80
60
40
20
50
30
12
10
8
6
4
2

Supplemental figure S1.

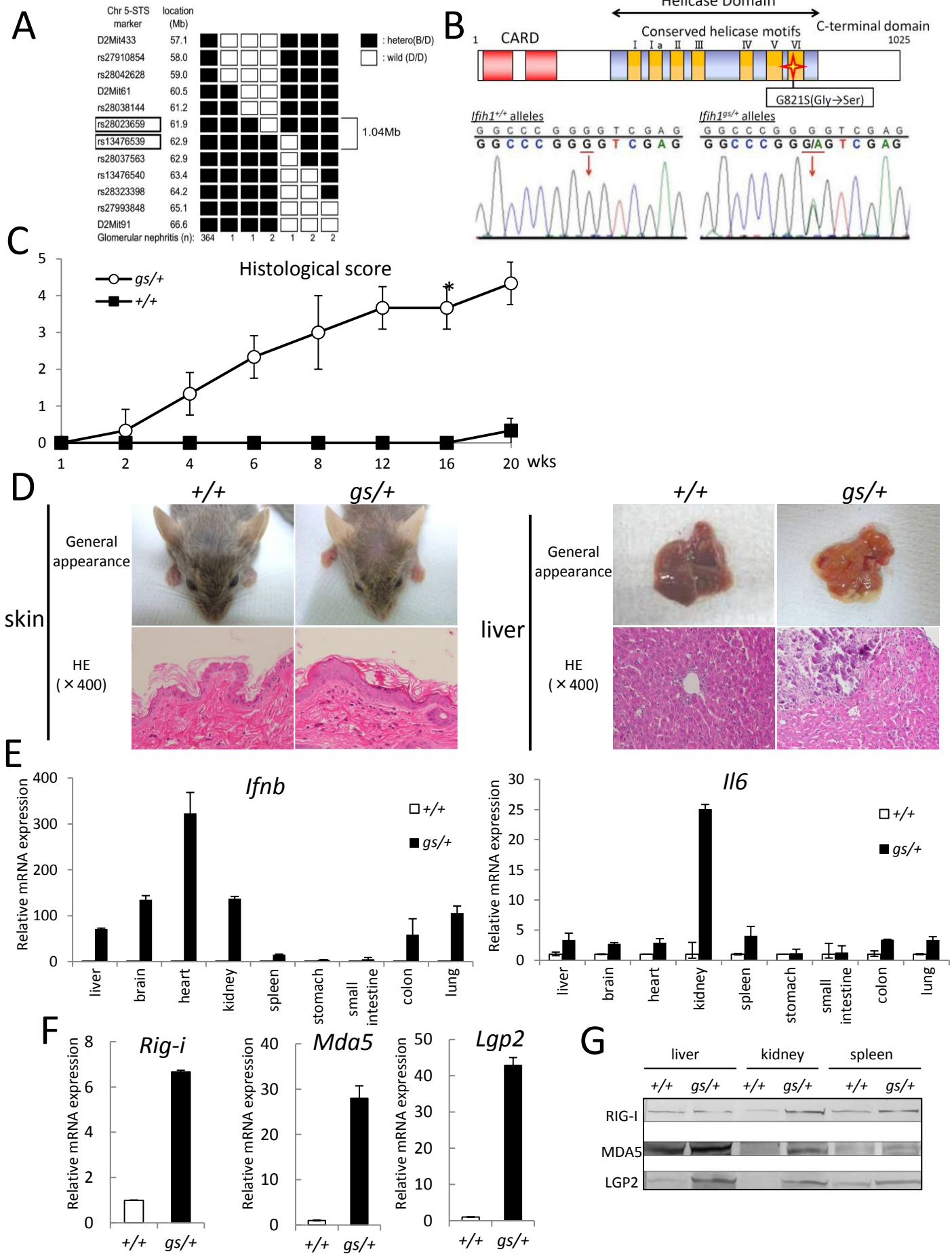

Supplemental figure S2.

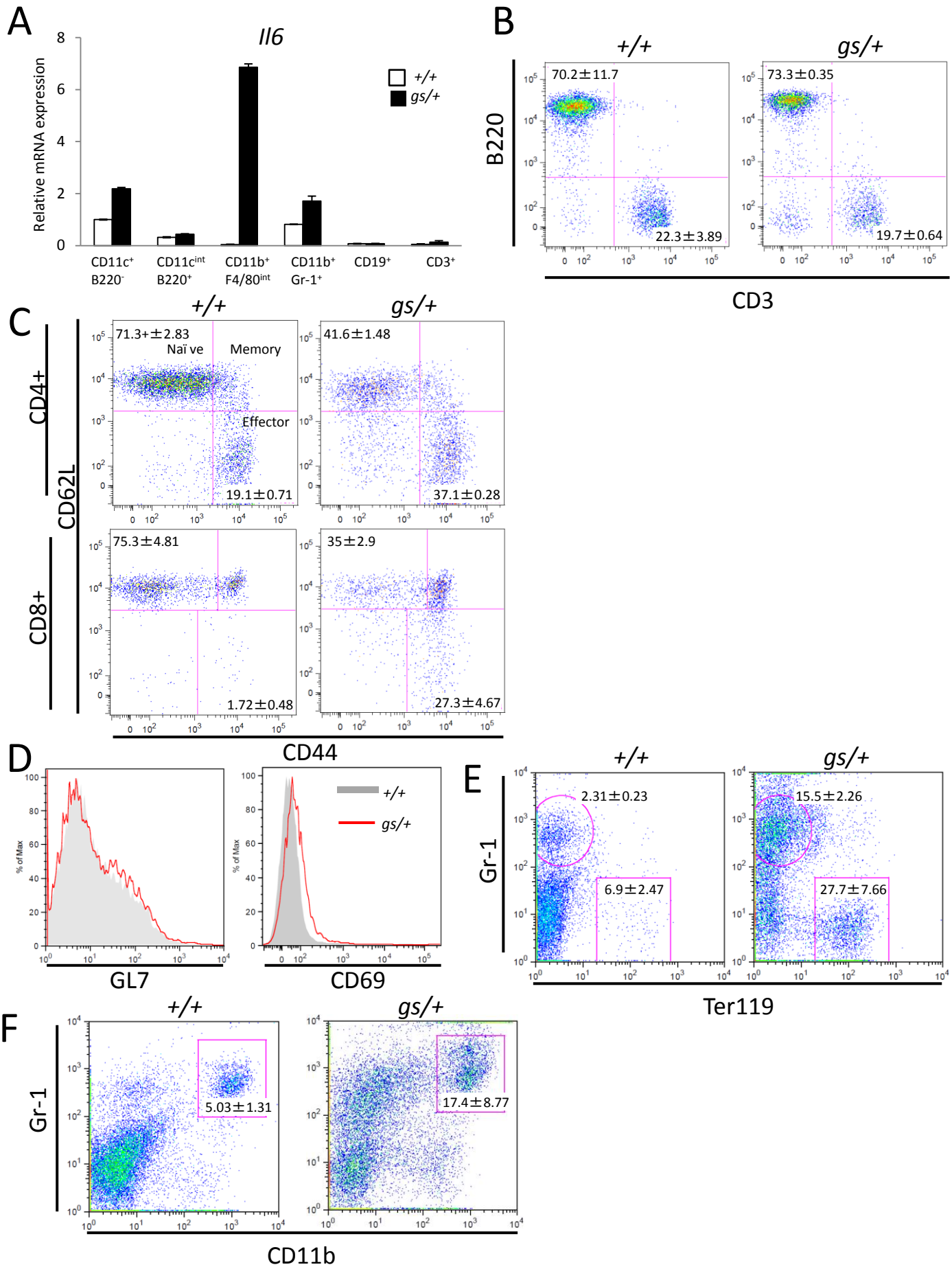

Supplemental figure S3.

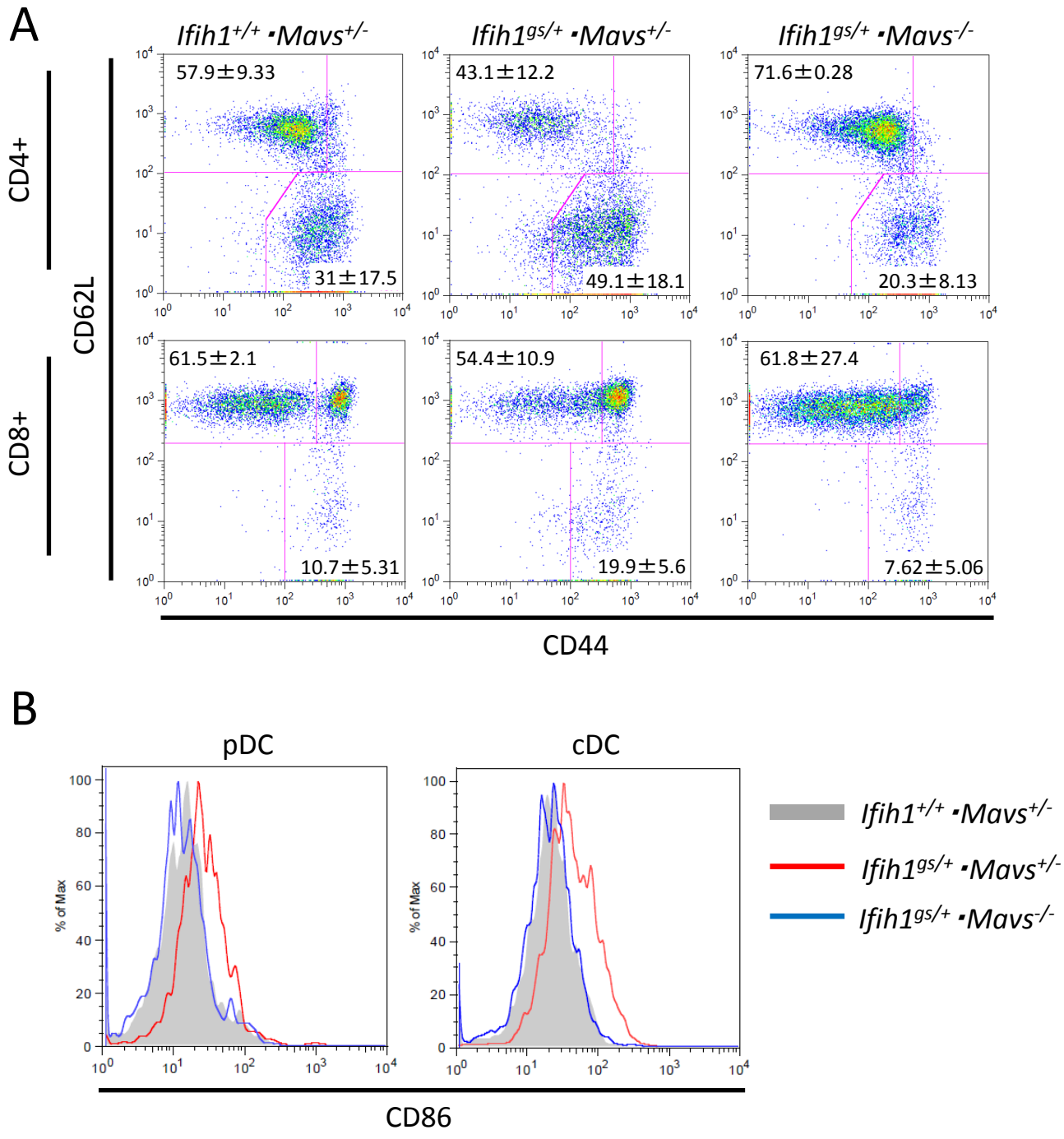

Figure 2.

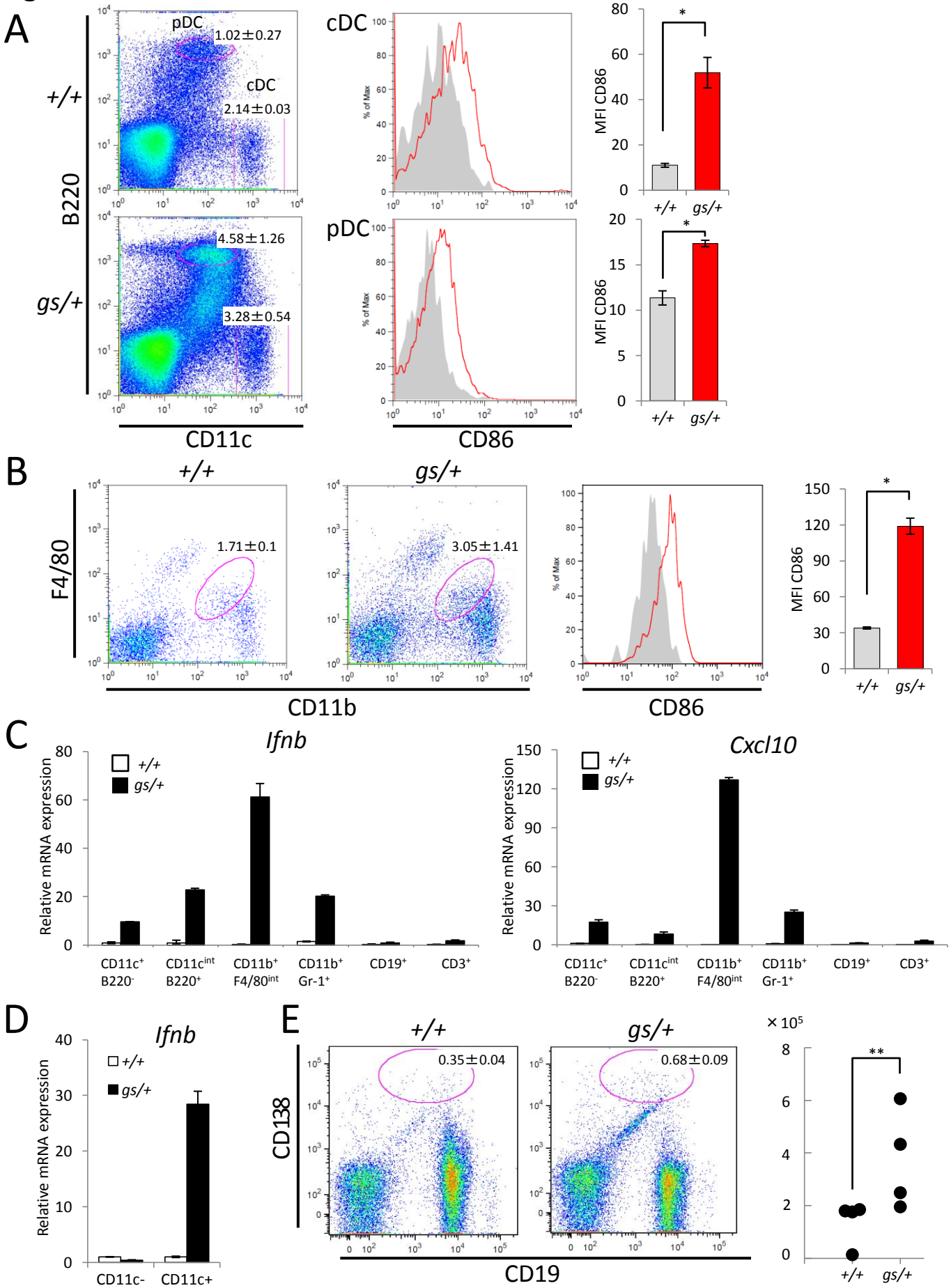
A
pDC
1.02±0.27
cDC
2.14±0.03
+/+
B220
4.58±1.26
gs/+
3.28±0.54
CD11c
cDC
pDC
% of Max
CD86
MFI CD86
+/+
gs/+
*
B
+/+
gs/+
F4/80
1.71±0.1
3.05±1.41
CD11b
CD86
MFI CD86
C
Ifnb
Cxcl10
+/+
gs/+
Relative mRNA expression
CD11c+ B220-
CD11cint B220+
CD11b+ F4/80int
CD11b+ Gr-1+
CD19+
CD3+
D
Ifnb
CD11c-
CD11c+
E
+/+
gs/+
CD138
0.35±0.04
0.68±0.09
CD19
×10^5
**

Figure 3.

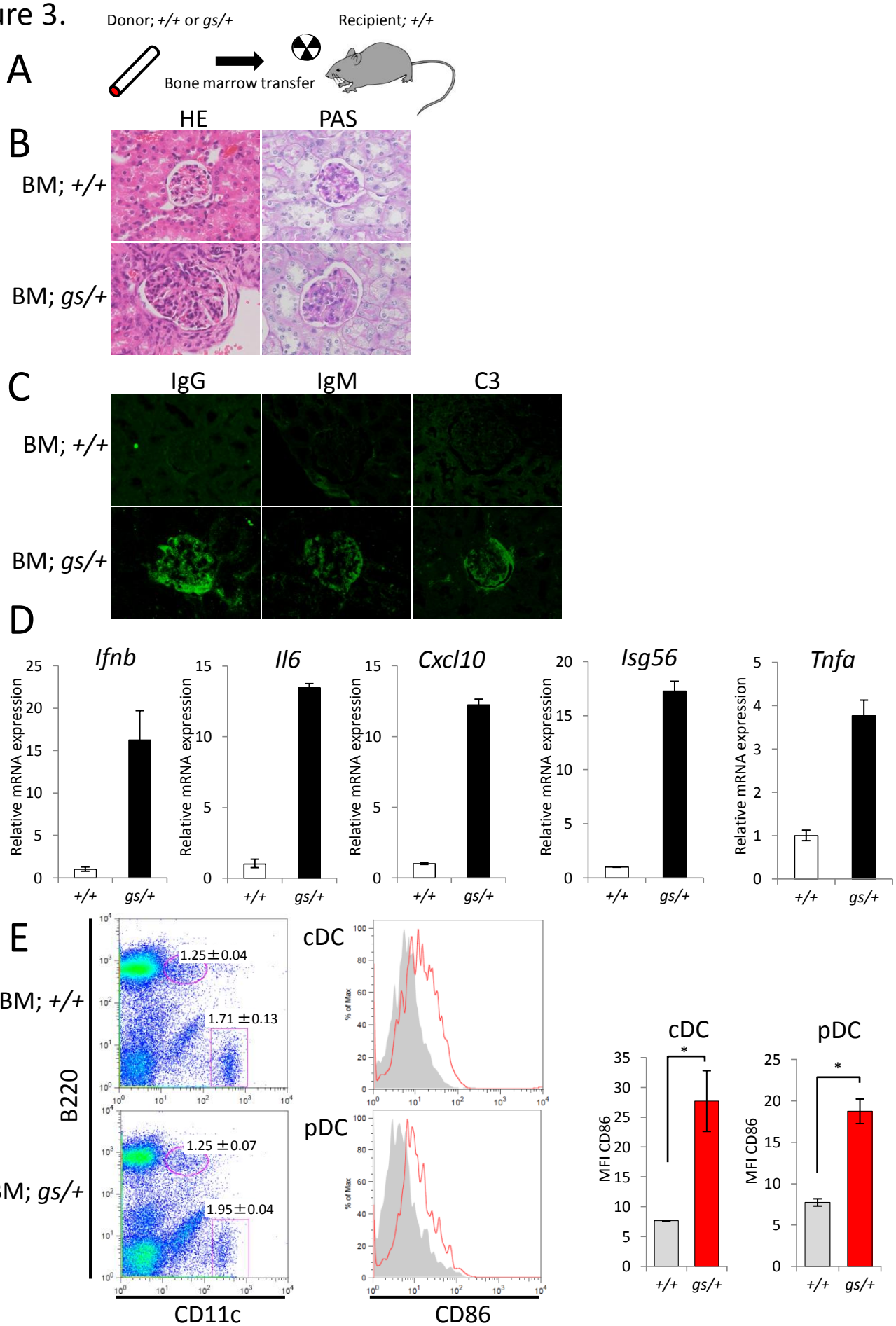
A
Donor; +/+ or gs/+
Recipient; +/+
Bone marrow transfer
B
HE
PAS
BM; +/+
BM; gs/+
C
IgG
IgM
C3
BM; +/+
BM; gs/+
D
Ifnb
Il6
Cxcl10
Isg56
Tnfa
Relative mRNA expression
+/+
gs/+
E
BM; +/+
BM; gs/+
B220
CD11c
1.25±0.04
1.71 ±0.13
1.25 ±0.07
1.95±0.04
cDC
pDC
% of Max
CD86
cDC
pDC
MFI CD86
*
*

Figure 4.

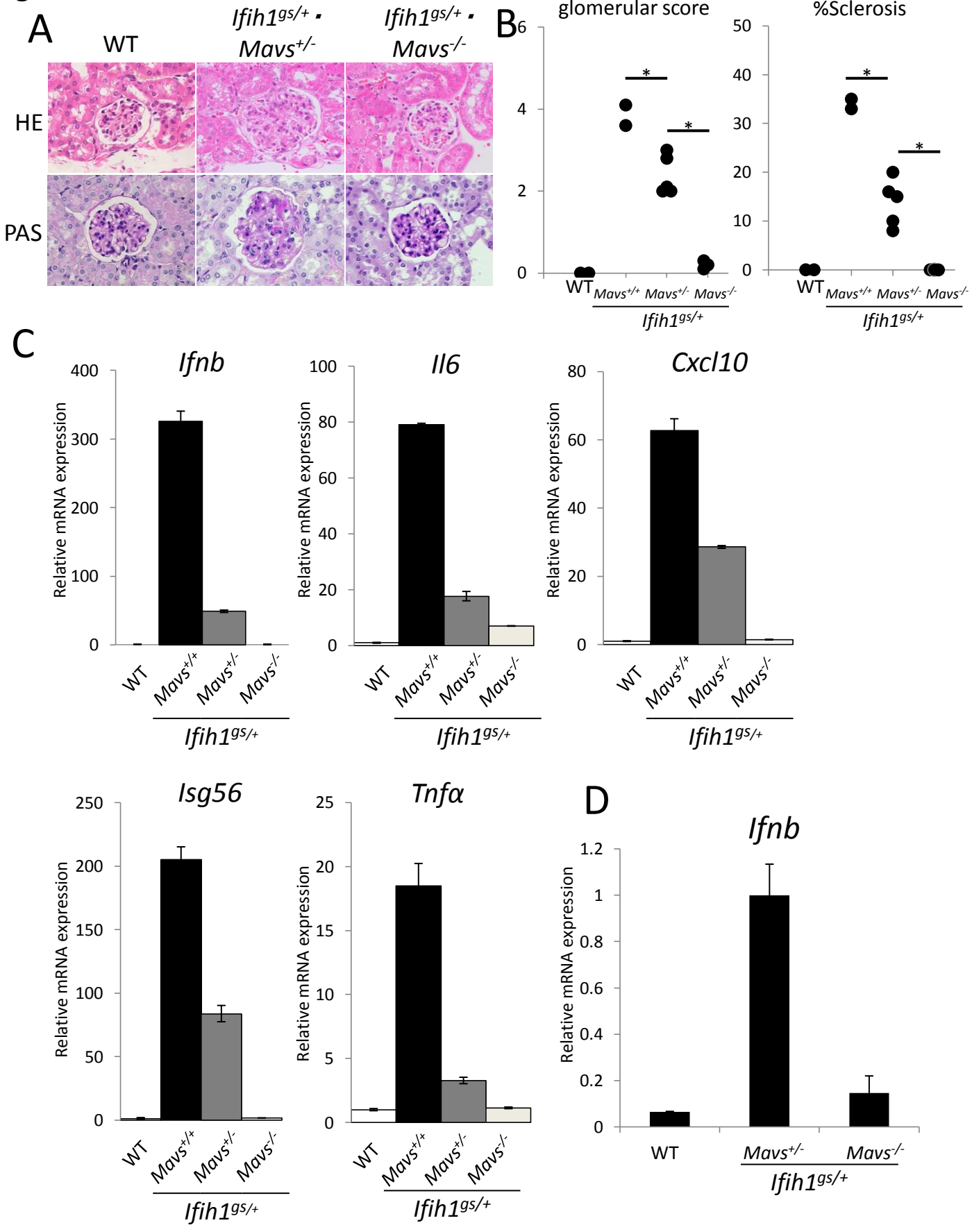
A
WT
Ifih1gs/+ · Mavs+/-
Ifih1gs/+ · Mavs-/-
HE
PAS
B
glomerular score
%Sclerosis
WT
Mavs+/+
Mavs+/-
Mavs-/-
Ifih1gs/+
C
Ifnb
Il6
Cxcl10
Isg56
Tnfα
Relative mRNA expression
D
Ifnb

Figure 5.

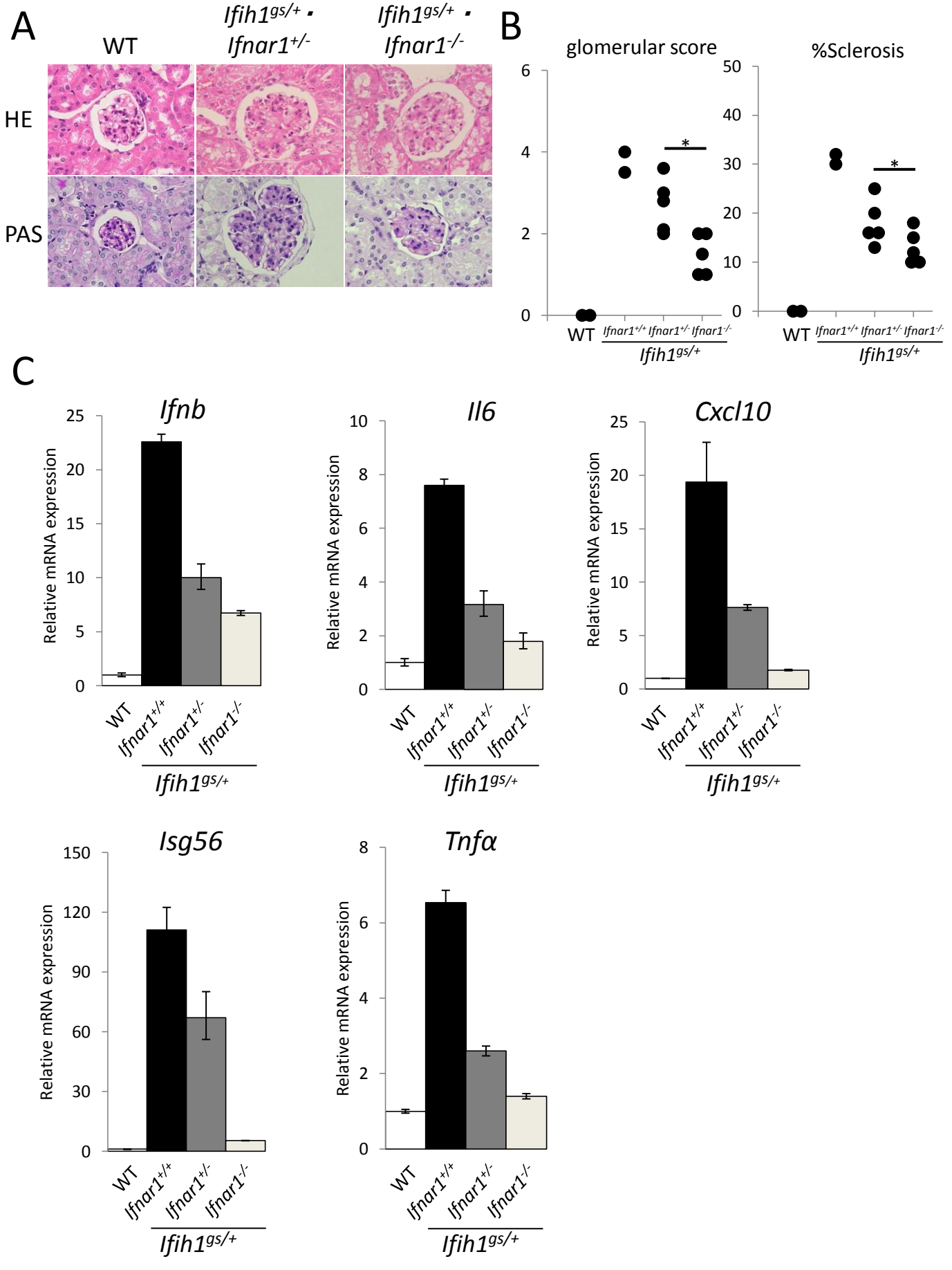
A
WT
Ifih1gs/+ · Ifnar1+/-
Ifih1gs/+ · Ifnar1-/-
HE
PAS
B
glomerular score
%Sclerosis
WT
Ifnar1+/+ Ifnar1+/- Ifnar1-/-
Ifih1gs/+
C
Ifnb
Il6
Cxcl10
Isg56
Tnfα
Relative mRNA expression
WT
Ifnar1+/+
Ifnar1+/-
Ifnar1-/-
Ifih1gs/+

Figure 6.

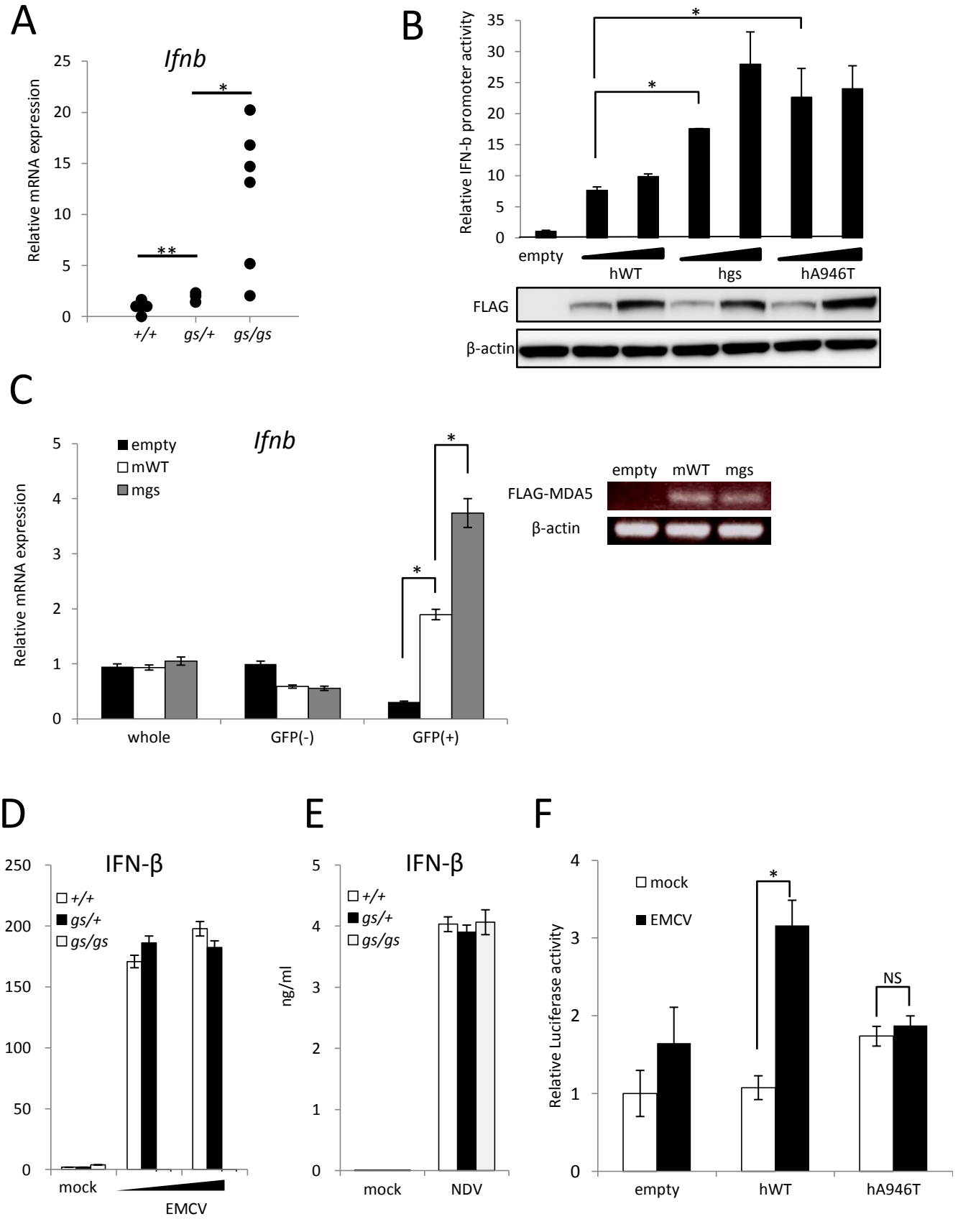
A
Ifnb
Relative mRNA expression
+/+
gs/+
gs/gs
B
Relative IFN-b promoter activity
empty
hWT
hgs
hA946T
FLAG
β-actin
C
Ifnb
empty
mWT
mgs
Relative mRNA expression
whole
GFP(-)
GFP(+)
FLAG-MDA5
β-actin
D
IFN-β
pg/ml
mock
EMCV
E
IFN-β
ng/ml
mock
NDV
F
mock
EMCV
Relative Luciferase activity
NS
empty
hWT
hA946T

Figure 7.

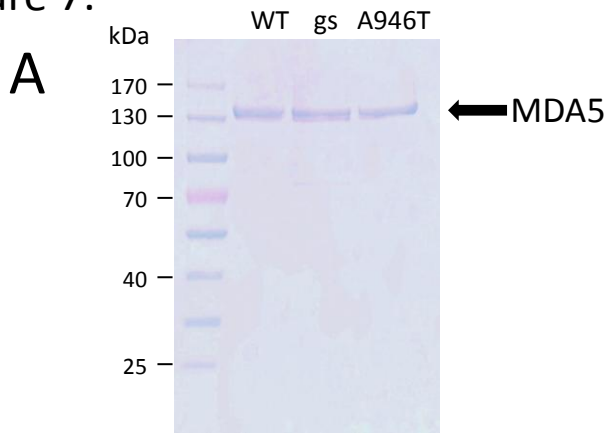
A
WT
gs
A946T
kDa
170
130
100
70
40
25
MDA5

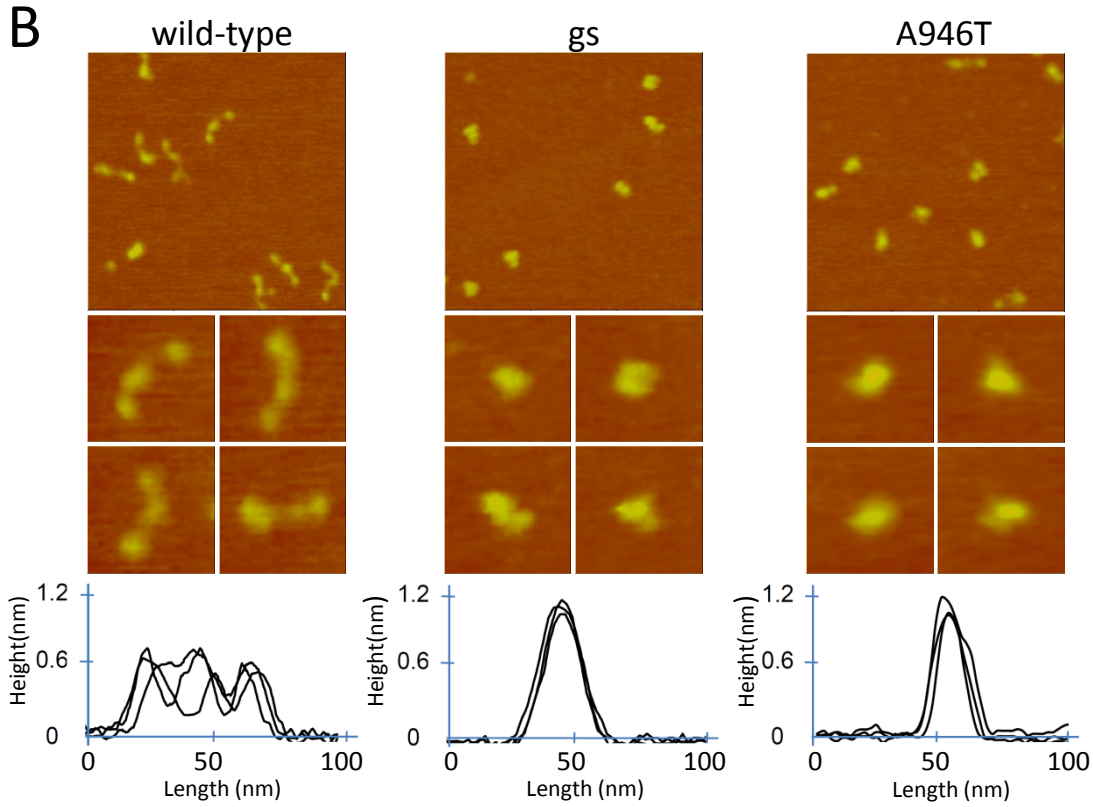
B
wild-type
gs
A946T
Height(nm)
1.2
0.6
0
0
50
100
Length (nm)

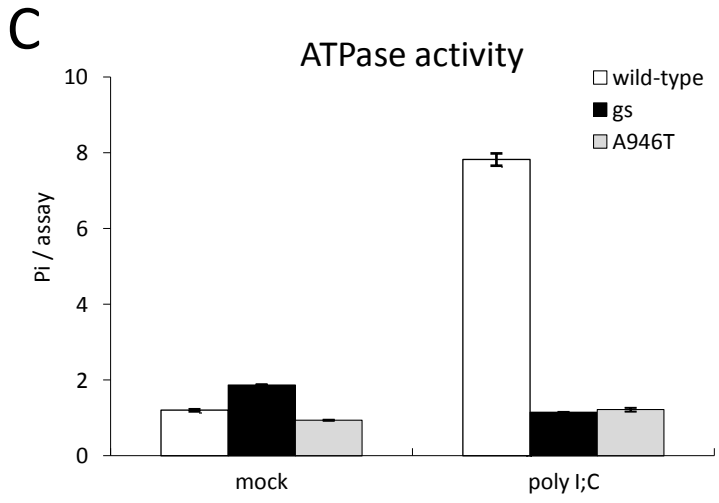
C
ATPase activity
wild-type
gs
A946T
Pi / assay
10
8
6
4
2
0
mock
poly I;C